the plant journal

SEB SOCIETY FOR EXPERIMENTAL BIOLOGY

The Plant Journal (2010) **62**, 160–170 doi: 10.1111/j.1365-313X.2009.04122.x

TECHNICAL ADVANCE

Proteasome activity profiling: a simple, robust and versatile method revealing subunit-selective inhibitors and cytoplasmic, defense-induced proteasome activities

Christian Gu[1], Izabella Kolodziejek[1,†], Johana Misas-Villamil[1,†], Takayuki Shindo[1], Tom Colby[3], Martijn Verdoes[2], Kerstin H. Richau[1], Jürgen Schmidt[3], Hermen S. Overkleeft[2] and Renier A. L. van der Hoorn[1,*]

[1]*Plant Chemetics Lab, Chemical Genomics Centre of the Max Planck Society, Max Planck Institute for Plant Breeding Research, 50829 Cologne, Germany,*

[2]*Leiden Institute of Chemistry and Netherlands Proteomics Centre, Gorlaeus Laboratories, 2333 CC Leiden, The Netherlands, and*

[3]*Mass Spectrometry Group, Max Planck Institute for Plant Breeding Research, 50829 Cologne, Germany*

Received 23 November 2009; accepted 10 December 2009; published online 1 February 2010.
[*]For correspondence (fax +49 221 5062 207; e-mail hoorn@mpiz-koeln.mpg.de).
[†]These authors contributed equally to this work.

SUMMARY

The proteasome plays essential roles in nearly all biological processes in plant defense and development, yet simple methods for displaying proteasome activities in extracts and living tissues are not available to plant science. Here, we introduce an easy and robust method to simultaneously display the activities of all three catalytic proteasome subunits in plant extracts or living plant tissues. The method is based on a membrane-permeable, small-molecule fluorescent probe that irreversibly reacts with the catalytic site of the proteasome catalytic subunits in an activity-dependent manner. Activities can be quantified from fluorescent protein gels and used to study proteasome activities *in vitro* and *in vivo*. We demonstrate that proteasome catalytic subunits can be selectively inhibited by aldehyde-based inhibitors, including the notorious caspase-3 inhibitor DEVD. Furthermore, we show that the proteasome activity, but not its abundance, is significantly increased in Arabidopsis upon treatment with benzothiadiazole (BTH). This upregulation of proteasome activity depends on NPR1, and occurs mostly in the cytoplasm. The simplicity, robustness and versatility of this method will make this method widely applicable in plant science.

Keywords: proteasome, Arabidopsis, vinyl sulfone, benzothiadiazole, activity-based protein profiling, papain-like cysteine proteases.

INTRODUCTION

Plants are able to adapt to changing environments and undergo drastic developmental changes. These processes require effective and selective protein turnover machinery. Turnover of most cytosolic and nuclear proteins is mediated by the ubiquitin/proteasome system (Sullivan *et al.*, 2003). This system is highly conserved in eukaryotes and is well studied in yeast. The 26S proteasome is a large multisubunit protease residing in the cytosol and nucleus and consists of a 20S core protease (CP) and a 19S regulatory particle (RP). The RP accepts ubiquitinated substrates, unfolds them and feeds them into the CP (Kurepa and Smalle, 2008).

The CP is structured as a 670 kDa hollow cylinder formed by four stacked rings of seven α and β subunits (Groll *et al.*, 1997). The proteolytic activity resides in three of the seven β subunits which are located in the inner cavity of the cylinder. Subunit β1 has caspase-like activity (cleaving after acidic residues); β2 has trypsin-like activity (cleaving after basic residues); and β5 has chymotrypsin-like activity (cleaving after hydrophobic residues) (Dick *et al.*, 1998). Together, these subunits degrade the substrate proteins into peptides of 3–20 amino acids that are released into the cytosol or nucleus.

Substrate specificity of the proteasome resides in selective ubiquitination of target proteins (Sullivan *et al.*, 2003), but the proteasome itself can also play regulatory roles. Proteasomes exist in subpopulations with different subunit compositions having different activities (Drews *et al.*, 2007). The mammalian immuno-proteasome, for example, releases hydrophobic peptides for antigen presentation (Rock *et al.*, 1994; Goldberg *et al.*, 2002). The catalytic subunits in Arabidopsis are encoded by *PBA1* (β1), *PBB1* and *PBB2* (β2) and *PBE1* and *PBE2* (β5) (Kurepa and Smalle, 2008). In tobacco, transcript levels encoding a β1 catalytic subunit are specifically upregulated during defense, suggesting the existence of 'plant defense proteasomes' (Suty *et al.*, 2003). That the plant proteasome plays a regulatory role in defense is exemplified by proteasome-mediated regulation of NPR1 (Spoel *et al.*, 2009) and that the proteasome is required for the avrRpm1-mediated hypersensitive response (HR) (Hatsugai *et al.*, 2009).

The development of tools to monitor the activity of the proteasome is instrumental for further studies. Monitoring proteasome activities during development and defense could lead to the identification of novel proteasome inhibitors and activators of endogenous or exogenous origin, as well as changes in the composition of the proteasome complex. Furthermore, subunit-specific inhibitors can be used to determine the role of each proteasome catalytic subunit.

Current methods to measure proteasome activities rely on using fluorogenetic subunit-selective substrates (e.g. Hatsugai *et al.*, 2009). Purification of the proteasome is required for these assays to exclude the conversion of fluorogenetic substrates by other proteolytic enzymes. Proteasome isolation and activity measurement is laborious and restricted to particular tissues since starch and polyphenols interfere in plant protein isolation (Yang *et al.*, 2004). Further research on the role of the proteasome in developmental and defense-related processes requires methods that are robust, simple and can be used to monitor proteasome activities in various plant organs without the need to disrupt the tissue and purify the proteasome.

Activity-based protein profiling (ABPP) is a powerful tool for monitoring the activity of enzymes in extracts and living cells (Cravatt *et al.*, 2008). Activity-based protein profiling involves activity-based probes (ABPs), which are biotinylated or fluorescent inhibitors that react with active site residues of enzymes in a mechanism-dependent manner, resulting in an irreversible covalent bond that facilitates the display of labeled enzymes on proteins gels, and the identification of labeled proteins by affinity capture and mass spectrometry. The accessibility of active sites in a proteome is a hallmark of enzyme activities (Kobe and Kemp, 1999). Activity-based protein profiling discriminates active proteins from their inactive isoforms since labeling only occurs with active enzymes, and ABPP thereby displays information on the functional state of enzymes rather than their abundance.

The potential of ABPP in plant science is illustrated with the introduction of DCG-04, an activity-based probe for papain-like cysteine proteases (PLCPs) (Greenbaum *et al.*, 2000). Since its introduction into plant science (van der Hoorn *et al.*, 2004) this probe has been used to reveal senescence-induced protease activities (Martinez *et al.*, 2007), defense-related protease activation (Gilroy *et al.*, 2007) and various pathogen-derived inhibitors that target tomato proteases (Rooney *et al.*, 2005; Tian *et al.*, 2007; van Esse *et al.*, 2008; Shabab *et al.*, 2008; Song *et al.*, 2009). The wide use of DCG-04 in medical research has caused commercialization of the probe, making it more accessible to the research community.

Activity-based probes based on vinyl sulfone (VS) reactive groups were shown to label the catalytic subunits of the mammalian proteasome (Kessler *et al.*, 2001; Verdoes *et al.*, 2006). To expand ABPP to study plant proteasome functions, we developed protocols to display activities of all three catalytic subunits of the Arabidopsis proteasome in crude plant extracts and *in vivo* using VS-based probes. This method facilitates the selection of subunit-specific inhibitors, and enables the display of activities of the different catalytic subunits during biological processes, as illustrated by the investigation of proteasome activities during defense responses.

RESULTS

Characterization of labeling

Two activity-based probes were used in this study (Figure 1a). Both probes carry a VS reactive group, a leucine tripeptide binding group and a long non-natural peptide linker. The probes differ, however, in the reporter tags. MV151 contains a Bodipy fluorescent group for fluorescent imaging (Verdoes *et al.*, 2006), whereas BioVS (previously called AdaK(Bio)Ahx$_3$L$_3$VS; Kessler *et al.*, 2001) contains a biotin tag for detection and affinity purification.

Labeling of Arabidopsis leaf extracts with 0.4 μM MV151 reveals three strong fluorescent signals at 25 kDa, and two weak signals at 30 and 40 kDa (Figure 1b, indicated by triangles and dots, respectively). As will be demonstrated later (Figure 2), the strong 25 kDa signals represent the three proteasome catalytic subunits whereas the weak 30 and 40 kDa signals represent PLCPs. All the fluorescent signals are suppressed by pre-incubation with 20 μM BioVS, indicating that BioVS competes for the same target proteins as MV151 (Figure 1b). Labeling of Arabidopsis leaf extracts with 2 μM BioVS also causes three signals at 25 kDa, and a few additional signals (Figure 1c). Many of these additional signals are also present in the no-probe control, indicating that these are caused by endogenously biotinylated proteins

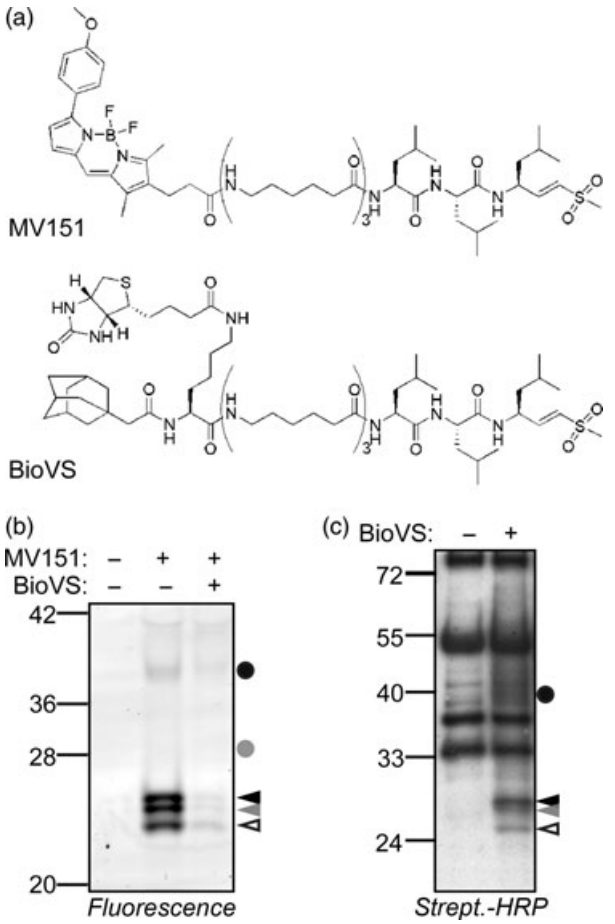

Figure 1. Labeling of Arabidopsis leaf extracts by vinyl sulfone (VS) probes.
(a) Molecular structures of the VS probes used in this study. Both probes carry a VS reactive group; a leucine tripeptide binding group; and a long linker region. MV151 carries a Bodipy fluorescent reporter tag. BioVS (also called AdaK(Bio)Ahx$_3$L$_3$VS; Kessler *et al.*, 2001) carries a biotin reporter tag and an adamantane to enhance membrane permeability.
(b, c) Labeling profiles of MV151 and BioVS. Arabidopsis leaf extracts were labeled for 3.5 h with 0.4 μM MV151 or for 2.5 h with 2 μM BioVS. Labeled proteins were detected on protein gel by fluorescence scanning (b) or on protein blot using streptavidin horseradish peroxidase conjugates (strept.-HRP). (c) Specific signals are indicated with circles and triangles. Pre-incubation with 20 μM BioVS prevents subsequent labeling by MV151 (b).

(Figure 1c). We chose to use MV151 labeling for activity profiling for the low background, ease of use and signal quantification.

MV151 targets the proteasome and PLCPs

To identify the labeled proteins, Arabidopsis leaf extracts were treated with BioVS. The resulting biotinylated proteins were purified on streptavidin beads and detected on a Coomassie-stained gel. Three signals at 25 kDa coincided with the three biotinylated signals detected by protein blotting (Figure 2a). These protein bands were excised, digested with trypsin and subjected to tandem mass spectrometry (MS). The MS data revealed that the upper signal represents the β2 catalytic subunit of the proteasome (PBB1, At3g27430), the middle signal represents subunit β5 (PBE1, At1g13060), and the lower signal subunit β1 (PBA1, At4g31300) (Figure 2b). There were no specific peptides identified from PBB2 and PBE2 in this analysis, but PBB2 was detected from the upper 25 kDa signal in a repetition experiment (data not shown). The identified peptides are all from the mature subunits and not from the prodomain, which is autocatalytically removed before the proteasome assembly (Heinemeyer *et al.*, 1997).

To independently demonstrate that PBA1 is amongst the purified biotinylated proteins, we used the PBA1 antibody (Yang *et al.*, 2004). Probing the purified BioVS-labeled proteins with this PBA1 antibody revealed a single strong signal at 23 kDa, demonstrating that the lowest of the three signals is indeed PBA1 (Figure 2a). Furthermore, western blot analysis of MV151-labeled proteomes with PBA1 antibody revealed a second signal at a slightly higher molecular weight, consistent with being MV151-labeled PBA1 (Figure 2c).

Analysis of proteins at the 30 and 40 kDa regions revealed peptides of PLCP RD21A (data not shown). The identification of PLCPs is consistent with our previous study identifying *in vivo* targets of MVA178, which is an azide-labeled version of MV151 (Kaschani *et al.*, 2008). *In vivo* labeling with MVA178 causes labeling at 30 and 40 kDa. Purification of these labeled proteins using click-chemistry revealed that the 40 kDa signal contains RD21A (At1g47128), whereas the 30 kDa signals contain RD21A, RD19A (At4g39090) and RD21C (At4g16190). This indicates that the signals detected with MV151 at 30 and 40 kDa are probably caused by labeling the same PLCPs.

To confirm that PLCPs are causing the 30 and 40 kDa signals in the MV151 labeling profile, we pre-incubated leaf extracts with and without E-64, which were then labeled with MV151 at pH 6.5 and 7.4. Pre-incubation with PLCP inhibitor E-64 prevented labeling at 30 and 40 kDa, and had no effect on labeling of the signals at 25 kDa (Figure 2d). To demonstrate that RD21A causes the signal at 40 kDa, we labeled extracts of leaves of the *rd21A-1* knockout line (Wang *et al.*, 2008). The 40 kDa signal is missing in extracts of the *rd21A-1* knockout line, confirming that this signal is caused by RD21A (Figure 2d). The signal at 30 kDa is reduced in the *rd21A-1* knockout line. This is consistent with the fact that RD21A exists as 30 and 40 kDa isoforms which are both active (Yamada *et al.*, 2001; van der Hoorn *et al.*, 2004). The remaining 30 kDa signals in the MV151 labeling profile of the *rd21A-1* lines are probably caused by RD19A or RD19C, or other PLCPs, since these PLCPs were found in this region during *in vivo* labeling with VS-based probes (Kaschani *et al.*, 2008).

To confirm that MV151 targets PLCPs, we pre-incubated leaf extracts with 40 μM MV151 and then labeled with

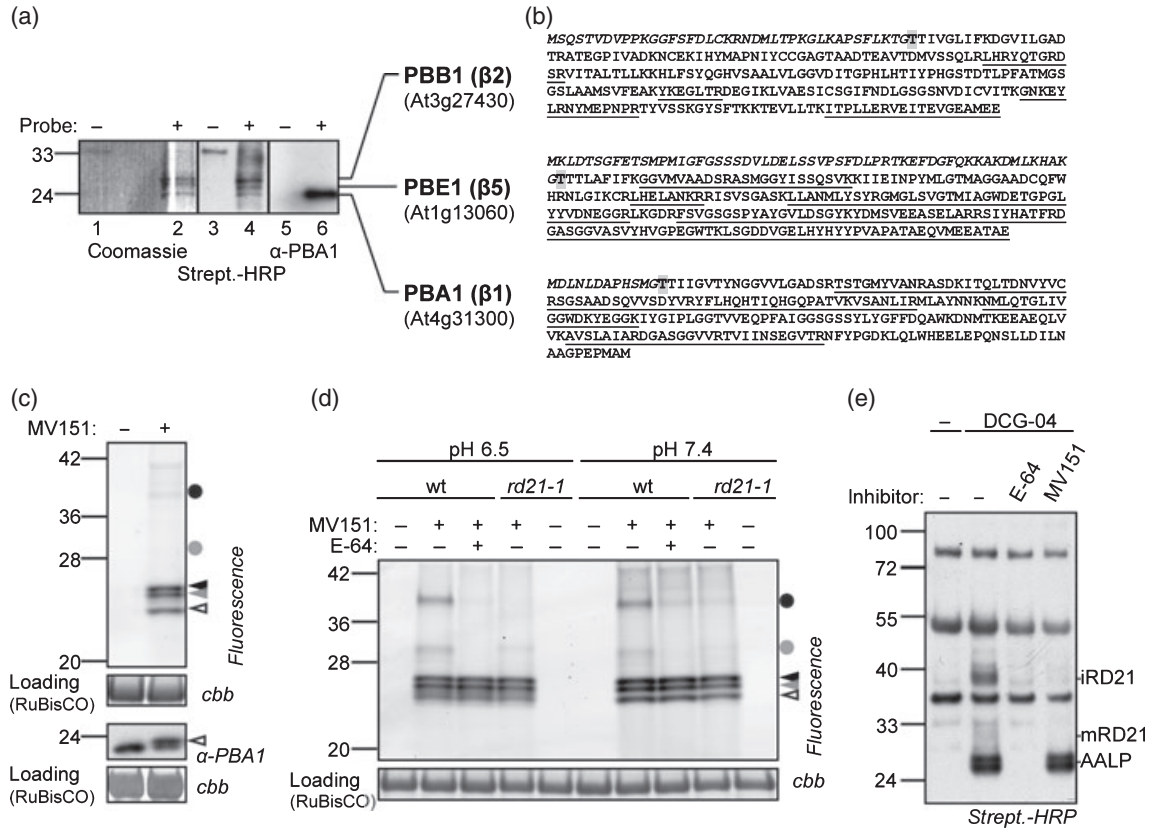

Figure 2. Identification and confirmation of the MV151-labeled proteins.
(a) The three 25 kDa signals represent the three catalytic β subunits of the proteasome. Arabidopsis leaf extract was labeled with BioVS and biotinylated proteins were purified, separated on protein gel and stained with Coomassie (left panel). Proteins from the three bands were digested by trypsin and analyzed by tandem mass spectroscopy (MS/MS). Proteins were identified as PBB1, PBE1 and PBA1, respectively (right). The identity of PBA1 was confirmed with a PBA1 antibody (right panel).
(b) Sequences of the three catalytic subunits with the identified peptides. Italics, prodomain; grey, boxed T, catalytic threonine; underlined, identified peptides.
(c) Labeling by MV151 causes a shift in gel migration of PBA1. Leaf extracts were labeled with 0.4 μM MV151 and proteins were detected by fluorescent scanning and PBA1 antibody.
(d) The 40 kDa signal is absent in the *rd21A-1* knockout line. Arabidopsis leaf extracts from wild-type (wt) and *rd21A-1* mutant plants were pre-incubated with or without 40 μM E-64 and labeled for 4.5 h with 0.4 μM MV151 at pH 6.5 and pH 7.4.
(e) MV151 prevents labeling of RD21A by DCG-04. Arabidopsis leaf extracts were pre-incubated with 40 μM MV151 and labeled with 2 μM DCG-04. Labeling of intermediate (i) RD21A is prevented by pre-incubation with MV151, whereas labeling of Arabidopsis aleurain-like protease (AALP) is not.

2 μM DCG-04, a biotinylated derivative of E-64 which labels PLCPs (Greenbaum *et al.*, 2000). Labeling with DCG-04 on Arabidopsis leaf extracts results in a typical activity-based profile containing intermediate (i) RD21A at 40 kDa, a mixture of various PLCPs at 30 kDa, and Arabidopsis aleurain-like protease (AALP) at 25 kDa (van der Hoorn *et al.*, 2004). Pre-incubation with E-64 prevents labeling of all these signals (Figure 2e). Interestingly, pre-incubation with MV151 prevents DCG-04 labeling of the 40 and 30 kDa signals but not of the 25 kDa AALP signal (Figure 2e), indicating that MV151 labels many PLCPs, but not all.

MV151 labeling was further characterized at various time points, probe concentrations, pHs and in the presence of other chemicals (Figures S1–S6). Labeling is saturated within 4 h (Figure S1) and at 1 μM MV151 (Figure S2). The profile is strongly pH dependent, with the three strongest proteasome signals at cytoplasmic pH (pH 7–8) (Figure S3). Labeling of the proteasome is not influenced by the presence of extra magnesium or calcium ions or NADPH (data not shown). Labeling of the weaker 30 and 40 kDa PLCP signals is stronger in 1 mM DTT (Figure S4), and the presence of 0.01 and 0.02% SDS prevents labeling of the β1 subunit whereas 0.1% SDS prevents labeling of all three subunits (Figure S5). Plant extracts contain the 20S proteasome since the RP–CP interaction requires ATP and the 26S proteasome stays intact by the addition of ATP during extraction (Yang *et al.*, 2004). However, adding ATP during extraction does not affect the MV151 labeling profile (Figure S6), suggesting that MV151 labels both the 20S and 26S proteasome.

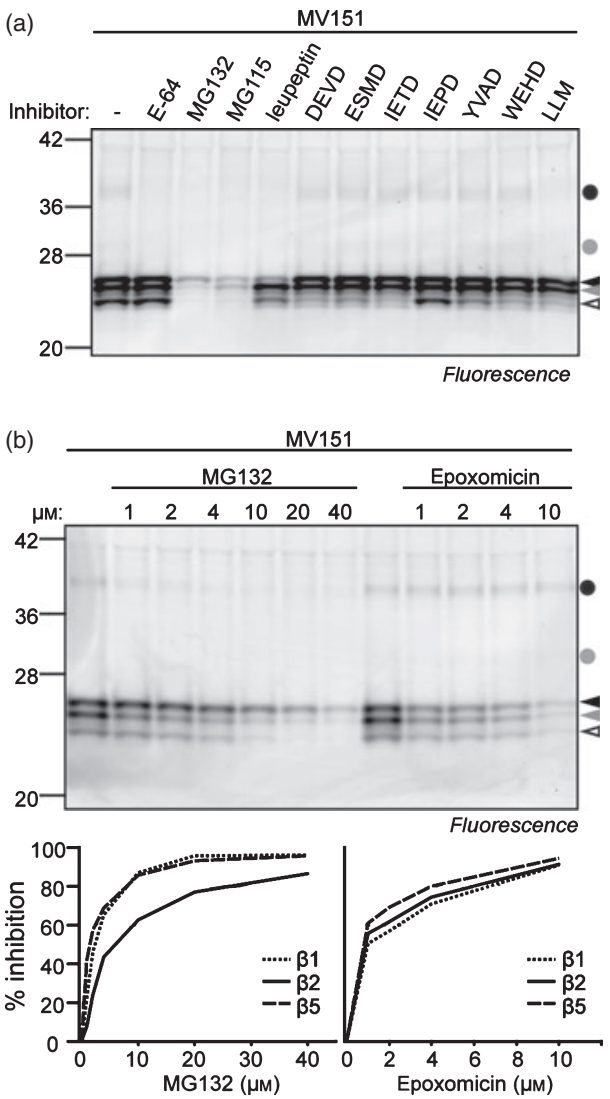

Figure 3. Selective inhibition of proteasome catalytic subunits.
(a) Inhibition of MV151 labeling. Arabidopsis leaf extract was pre-incubated with various inhibitors (50 μM) and then labeled with MV151 (0.5 μM). Fluorescent signals indicate the absence of inhibition.
(b) Concentration dependence of inhibition. Arabidopsis leaf extracts were pre-incubated at different concentrations of MG132 and epoxomicin and then labeled for 2 h with 0.4 μM MV151. Fluorescently labeled proteins were detected on protein gels by fluorescence scanning. Proteasome-derived signals were quantified and plotted against the inhibitor concentration in dose–response graphs (bottom).

Caspase inhibitors and other peptide aldehydes are subunit-selective proteasome inhibitors

We next tested whether MV151 labeling can be used to identify subunit-specific inhibitors. MG132 is a tri-leucine (LLL) aldehyde and a frequently used proteasome inhibitor in plant science. Pre-incubation of leaf extracts with MG132 followed by labeling with MV151 demonstrates that MG132 blocks MV151 labeling of β1 and β5 subunits and suppresses labeling of the β2 subunit (Figure 3a). Importantly, MG132 also prevents labeling of the 40 kDa RD21A, indicating that MG132 is not selective for the proteasome but also inhibits PLCPs. Pre-incubation with the PLCP inhibitor E-64 prevents MV151 labeling of the 40 kDa RD21A signal, but not the proteasome-derived signals (Figure 3a), consistent with the presumed high selectivity of E-64 (Powers *et al.*, 2002).

The availability of many commercial peptide aldehyde-based inhibitors and the observation that MG132 only partially inhibits the β2 subunit, prompted us to test other peptide aldehydes for selective inhibition of the proteasome. These inhibitors all carry a C-terminal aldehyde but differ in the residues of the peptide. Many of these peptide aldehyde-based inhibitors are designed to inhibit caspases, which are selective for aspartate (D) at the P1 position of the inhibitor. Pre-incubation with these inhibitors was followed by MV151 labeling to reveal the remaining activities (Figure 3a).

Interestingly, many of the caspase inhibitors prevent MV151 labeling of the β1 subunit (Figure 3a). This is consistent with the caspase-like activity of this subunit, and implies the involvement of the proteasome in various types of PCD in plants (Bonneau *et al.*, 2008). Labeling of the β1 subunit can also be blocked by LLM (Figure 3a), which carries a methionine (M) at the P1 position. Furthermore, IEPD is not effective in inhibition of β1, but IETD is, indicating that the proline (P) at the P2 position prevents inhibition of the β1 subunit. Labeling of the β2 subunit can be prevented by leupeptin (LLR), which is a frequently used PLCP inhibitor (Figure 3a), and was originally described as a proteasome inhibitor (Wilk and Orlowski, 1980). The fact that leupeptin can suppress labeling of the β2 subunit is consistent with the presumed trypsin-like activity (cleaving after basic residues) of the β2 subunit, since leupeptin carries an arginine (R) at the P1 position. Labeling of the β5 subunit can only be inhibited with MG132 and MG115 (LLNva) (Figure 3a). This is consistent with the presumed chymotrypsin-like activity (cleaving after hydrophobic residues) of the β5, since MG132 carries a leucine and MG115 a norvaline (Nva) at the P1 position. Finally, labeling of the 40 kDa RD21A signal can be prevented by E-64, MG132, MG115, leupeptin and LLMcho, but not by caspase inhibitors (Figure 3a). This is consistent with the fact that PLCPs like RD21A are selective for substrates having hydrophobic residues at the P2 position.

A dilution series of MG132 confirms that MG132 preferentially inhibits β5 and β1 (Figure 3b). Pre-incubation with the selective proteasome inhibitor epoxomicin (Meng *et al.*, 1999) also prevents MV151 labeling of all three subunits, but not of 40 kDa RD21A (Figure 3b). Quantification of the signals from an epoxomicin dilution series indicates that epoxomicin inhibits β1, β2 and β5 with similar affinities (Figure 3b).

MV151 labels cytoplasmic and nuclear proteasomes and PLCPs *in vivo*

To demonstrate that MV151 labeling can be used to monitor protein activities *in vivo*, we incubated Arabidopsis cell cultures with MV151. Two hours' incubation is enough to cause labeling of the proteasome subunits (mainly the β2 and β5 subunits), and PLCPs at 30 and 40 kDa (Figure 4, first lane), without affecting cell viability. The PLCP signals are relatively strong, compared with *in vitro* labeling (Figures 1–3).

To show that MV151 labeling can be used to monitor activities *in vivo* and to confirm the identity of the signals, we pre-incubated the cell culture with an excess of cell permeable inhibitors and then labeled with MV151. Pre-incubation with the PLCP inhibitor E-64d prevents labeling of the 30 and 40 kDa signals, whereas the proteasome inhibitor epoxomicin suppresses labeling of the 25 kDa signals, consistent with their identity. These experiments demonstrate that MV151 labeling can be used to monitor *in vivo* inhibition with selective inhibitors.

To determine the subcellular location of the labeled proteins, we separated the total extract (T) into a nuclear depleted (ND) and a nuclear enriched (NE) fraction. Western blotting with PBA1 antibody indicated that the proteasome occurs in both the ND and NE fractions, consistent with its location in the cytoplasm and nucleus, respectively (Figure 4). Since the NE fraction is 20-fold concentrated but the anti-PBA1 signals are similar in intensity, it can be concluded that about 5% of the cellular proteasome in cell cultures resides in the nucleus. A similar distribution occurs with the 25 kDa fluorescent proteasome signals, indicating that the nuclear and cytoplasmic proteasomes have similar activities (Figure 4). The majority of the PLCPs reside in the ND fraction, but a significant signal is in the NE fraction, suggesting that some of the PLCPs are localized in the nucleus. Taken together, these data demonstrate that MV151 can be used to monitor the activities of the proteasome and PLCPs in living cells at different subcellular locations.

Proteasome activity is induced during defense

To investigate if proteasome activities change during defense, we sprayed Arabidopsis plants with and without benzothiadiazole (BTH), which induces the salicylic acid (SA) signaling pathway (Kohler *et al.*, 2002). Extracts from water- and BTH-treated plants were subjected to MV151 profiling. Interestingly, BTH treatment results in increased activity of the proteasome. This upregulation is not associated with altered β1/β2/β5 signal ratios or sizes, occurs at 1 day after BTH treatment and remains for at least 5 days (Figure 5a). Although the upregulation is moderate, it occurs consistently in independent leaves and in different biological replicates (Figure 5b). Quantification showed a 1.46 ± 0.17 ($n = 7$) fold upregulation of the 25 kDa signals, and is statistically significant (Student's *t*-test: $P = 0.000013$). Western blot analysis shows equal levels of PBA1, indicating that the proteasome levels are equal between water- and BTH-treated plants and that BTH-induced activation caused an increased activity of the proteasome, rather than an increased abundance (Figures 5c and S7).

To further demonstrate the increased activity of the proteasome, we analyzed MV151-labeled extracts with the PBA1 antibody. The two signals on the anti-PBA1 western blot represent the active proteasome (upper signal) and inactive proteasome (lower signal). Interestingly, the ratio between the upper and lower signal increases upon BTH-treatment (Figures 5d and S8), supporting the hypothesis

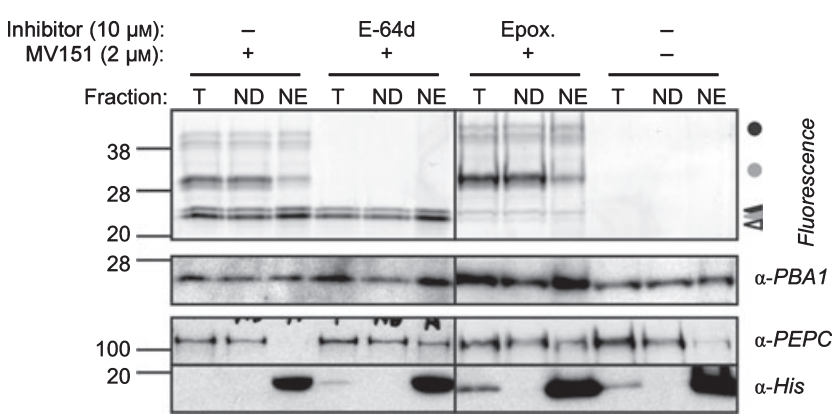

Figure 4. MV151 labels the nuclear and cytoplasmic proteasome *in vivo*.
Arabidopsis cell cultures were pre-incubated with 10 μM E-64d or epoxomicin for 30 min and labeled with 2 μM MV151 for 2 h. Cells were homogenized and total extracts (T) were separated into nuclear depleted (ND) and nuclear enriched (NE) fractions. Fluorescent proteins were detected by in-gel fluorescence scanning, and proteasome subunit PBA1, cytoplasmic marker PEPC and nuclear marker histone were detected by western blot on the same samples. The β1 subunit (the lowest of the three proteasome signals) is not labeled because of relatively short labeling times. Presence of PEPC in the nuclear fraction occurs with inhibitor-treated cells, and is probably caused by reduced cell viability at the time of sample processing.

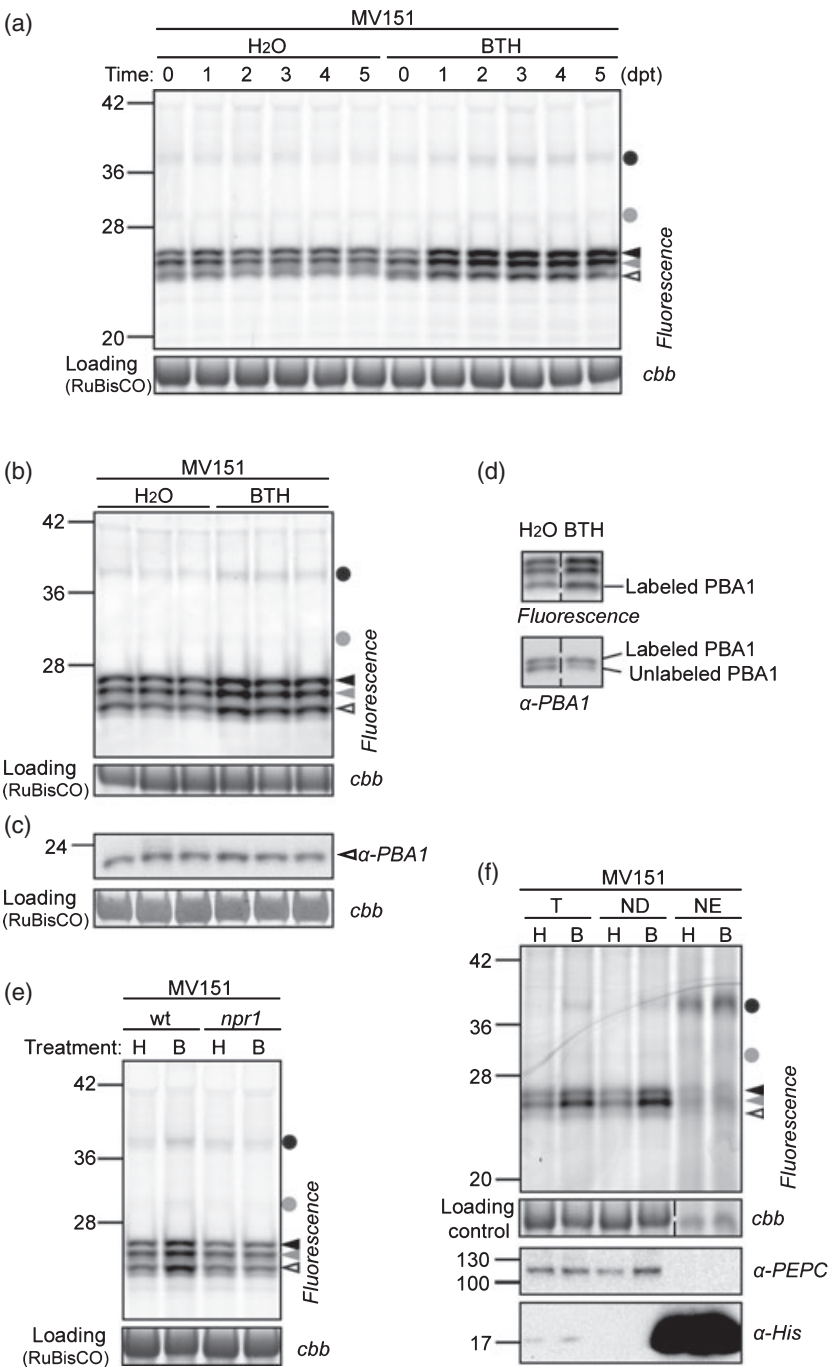

Figure 5. Upregulated proteasome activities in benzothiadiazole (BTH)-treated plants

(a) Time course of BTH-induced proteasome activity. Arabidopsis plants were sprayed with water or BTH and leaf extracts were labeled with MV151 at different days after treatment (dpt) with BTH.

(b) Reproducibility of BTH-induced proteasome activities. Three different pots each with four plants were sprayed with water or BTH. At 48 h post-treatment, extracts of four leaves from each pot were labeled with MV151. Shown is a representative of three biological replicates.

(c) Proteasome activation occurs post-translationally. Unlabeled extracts from (b) were detected with anti-PBA1 antibody.

(d) The proportion of active proteasome increases upon BTH treatment. Extracts of plants at 5 days after BTH treatment were labeled with MV151 and detected by fluorescence scanning (top) and western blotting with PBA1 antibody (bottom). The upper signal represents the active proteasomes that could be labeled with MV151.

(e) The BTH-induced proteasome activity is NPR1 dependent. Wild-type and *npr1* mutant plants were treated with water (H) or BTH (B) and leaf extracts were labeled with MV151.

(f) Proteasome activation occurs in the cytoplasm. Cell extracts (T) from water- and BTH-treated plants were separated into nuclear depleted (ND) and nuclear enriched (NE) fractions, and labeled with MV151. The NE extract was 80-fold more concentrated than the T and ND fractions. Anti-PEPC and anti-histone antibodies were used as markers for cytoplasmic and nuclear proteins, respectively.

that the activity of the proteasome but not the number of proteasomes is increased upon BTH treatment.

To show that the elevated proteasome activity in BTH-treated plants depends on the SA signaling pathway, we investigated BTH-induced proteasome activities in the Arabidopsis SA signaling mutant *npr1*. When *npr1* mutant plants were treated with BTH, proteasome activities were elevated in the wild type but not in *npr1* lines (Figure 5e). These data show that proteasome activity is not directly induced by BTH but requires NPR1 function, indicating that elevated proteasome activities are a response to activation of the SA signaling pathway.

To investigate in which cellular compartment the increased proteasome activity resides upon BTH treatment, we fractionated extracts from water- and BTH-treated plants in a ND and NE fraction and subjected those to MV151 profiling. Subcellular markers phosphoenolpyruvate carhoxylase (PEPC) and histone H3 confirmed that the

fractions were not cross-contaminated (Figure 5f). The increased level of PEPC upon BTH treatment is consistent with the BTH inducibility of this gene (http://www.genevestigator.com/; Zimmermann *et al.*, 2004; von Rad *et al.*, 2005). Labeling of the proteasome in the NE fraction did not occur, presumably because of improper labeling conditions. However, the ND fraction, containing over 90% of the cellular proteasomes, showed elevated labeling upon BTH treatment (Figure 5f). Thus, although we do not exclude BTH-induced activity in the nucleus, the majority of the BTH-induced proteasome activity resides in the cytoplasm.

DISCUSSION

We showed that VS-based probes can be used to monitor the activity of all three catalytic subunits of the proteasome and PLCPs. Since this method is based on labeling living tissues or crude extracts with fluorescent probes, followed by detection of fluorescently labeled proteins, this method is easier and more robust than traditional assays that include the purification of the proteasome and measurement of its activity using fluorogenic substrates. A single reaction is enough to simultaneously display the activities of all three catalytic subunits and some PLCPs. In-gel scanning of the fluorescently labeled proteome is also quantitative and quicker than western-blot analysis.

Simultaneous activity-based profiling of the three catalytic subunits and PLCPs is a powerful tool for testing the selectivity of protease and proteasome inhibitors. When testing different commercially available inhibitors, we found a striking inconsistency with the advertised selectivity. For example, proteasome inhibitors MG132 and MG115 also target PLCPs, and the PLCP inhibitor leupeptin and various caspase inhibitors also target the proteasome. That caspase-3 inhibitors target the β1 subunit is an interesting observation. Many caspase inhibitors block various types of programmed cell death (PCD) in plants (Bonneau *et al.*, 2008). However, plant genomes do not encode for caspases, so the target of these caspase-3 inhibitors remained elusive. Our data suggest that caspase-3 inhibitors act by targeting the β1 subunit of the proteasome, implicating the involvement of the proteasome in a diverse range of PCD processes in plants.

Inhibition assays with aldehyde-based inhibitors that differ only in the amino acid residues revealed data that are consistent with the knowledge that PLCPs are selective for hydrophobic residues at the P2 position, whereas the proteasome catalytic subunits are selective for residues at P1: β1 for acidic residues, β2 for basic residues, and β5 for hydrophobic residues (Heinemeyer *et al.*, 1997). The ability to use subunit-selective inhibitors has tremendous potential since these inhibitors would enable the determination of subunit-specific functions of the proteasome. Functional knockout studies cannot be achieved by genetics since mutations in the CP particle subunits are lethal (Kurepa and Smalle, 2008).

Activity-based protein profiling with MV151 revealed that proteasome activities are upregulated in BTH-treated plants in an NPR1-dependent manner. This was unexpected, since transcript levels of genes encoding proteasome subunits are unaltered upon BTH treatment (http://www.genevestigator.com/, Zimmermann *et al.*, 2004; von Rad *et al.*, 2005). Our data suggest that the upregulated proteasome activity is caused by a change in the proportion of active proteasomes. The mechanism of this BTH-induced activation of the proteasome is unknown at this point. However, it is well-described that the plant proteasome can be post-translationally regulated by, for example, oxidation of proteasome subunits (Basset *et al.*, 2002).

The upregulated proteasome activity is in line with a role of the proteasome in various defense responses. The avrRpm1-induced hypersensitive response requires proteasome activity (Hatsugai *et al.*, 2009) and induction of NPR1-regulated genes requires degradation of phosphorylated NPR1 by the proteasome (Spoel *et al.*, 2009). Furthermore, *Pseudomonas syringae* pv. *syringae* (*Pss*) produces the proteasome inhibitor Syringolin A (SylA) which contributes to its virulence (Groll *et al.*, 2008). We used ABPP to demonstrate that the proteasome is inhibited during *Pss* infection and that SylA can move systemically through the leaf to suppress the proteasome at sites distant from the bacterial colony (JM-V, IK and RALvdH, unpublished data). Besides regulatory roles, the proteasome may also play a role in releasing amino acids for the synthesis of defense-related proteins and compounds, and protect cells against reactive oxygen species and pathogen-inflicted damage. Benzothiadiazole causes a severe change in metabolism to generate defense-related proteins and compounds (Dietrich *et al.*, 2004). We speculate that an increased proteasome activity in the cytoplasm is required for efficient, large-scale proteolytic processes during defense. Defense-related proteasomes may even have different enzymatic activities, similar to mammalian 'immunoproteasomes' which releases hydrophobic peptides for antigen presentation (Rock *et al.*, 1994; Goldberg *et al.*, 2002). Interestingly, plant defense proteasomes are thought to occur in tobacco where transcript levels encoding a β1 catalytic subunit is specifically upregulated during elicitation (Suty *et al.*, 2003). The properties and role of defense-induced proteasome activities will be the subject of future studies.

In conclusion, proteasome activity profiling is a simple and robust method to discover changes in proteasome activities. This method will significantly support our future analysis of proteasome activities during pathogen infection, and is now available to the plant research community for the study of proteasome activities in a wide range of biological processes.

EXPERIMENTAL PROCEDURES

MV151 and BioVS

Synthesis of MV151 and BioVS has been described previously (Kessler *et al.*, 2001; Verdoes *et al.*, 2006). Aliquots of the probes are available upon request.

Plant materials

Arabidopsis thaliana ecotype Columbia plants were grown in a growth chamber at 24°C (day)/20°C (night) under a 12-h light regime. Rosette leaves of 4–6-week-old plants were used for protein extraction. The *rd21A-1* knockout line was described previously (Wang *et al.*, 2008). The BTH treatment was done by spraying 4-week-old plants with 300 μM BTH (Actigard; Syngenta, http://www.syngenta.com/). Samples were taken at various days after spraying with BTH.

Sample preparation, probe labeling and protein work

Proteins were extracted by grinding one rosette leaf in an Eppendorf tube. The extract was mixed with 0.5 ml of water and cleared by centrifugation (1 min at 16 000 ***g***). Labeling was usually done by incubating ~100 μg protein in 0.5 ml containing 50 mM 2-amino-2-(hydroxymethyl)-1,3-propanediol (TRIS) buffer (pH 7.4) and 0.4 μM MV151 for 3–4 h at room temperature (22–25°C) in the dark under gentle agitation. Equal volumes of DMSO were added to the no-probe controls. Proteins were precipitated after labeling by adding 1 ml of ice-cold acetone and subsequent centrifugation for 1 min at 16 000 ***g***. The pellet was dissolved in 2 × SDS-PAGE loading buffer containing β-mercaptoethanol, and separated on 12% SDS gels (~10 μg protein per lane). Labeled proteins were visualized by in-gel fluorescence scanning using a Typhoon 8600 scanner (GE Healthcare Life Sciences, http://www.gelifesciences.com) with excitation and emission at 532 and 580 nm, respectively. Fluorescent signals were quantified with ImageQuant 5.2 (GE Healthcare Life Sciences). Alternatively, protein extracts were labeled with 2 μM BioVS in 50 mM TRIS buffer (pH 8) and 1 mM DTT or with 2 μM DCG-04 in 50 mM sodium acetate buffer (pH 6) and 1 mM DTT. After SDS PAGE, proteins were transferred onto polyvinylidene fluoride membrane (Immobilon-P; Millipore, http://www.milliporecom/) and detected using streptavidin-horseradish peroxidase (HRP) (1:3000; Ultrasensitive, Sigma, http://www.sigmaaldrich.com/) or anti-PBA1 antibodies (1:5000; BIOMOL, http://www.enzolifesciences.com/biomol/), combined with HRP-conjugated anti-rabbit secondary antibodies (1:5000). Profiling at various pH values was done using 50 mM sodium acetate (pH 4–6.5) or TRIS (pH 7–11) buffers. Competition or inhibition assays were done by pre-incubating the protein extracts with competitor or inhibitor molecules for 30 min before labeling with activity-based probes.

In vivo labeling and nuclear fractionation

Cell cultures (Arabidopsis ecotype Landsberg; May and Leaver, 1993) were weekly subcultured in medium [3% w/v sucrose, 0.5 mg L^{-1} naphthalene acetic acid, 0.05 mg L^{-1} 6-benzylaminopurine (BAP) and 4.4 g MS Gamborg B5 vitamins (Duchefa, http://www.duchefa.com/), pH 5.7]. Before labeling, 6 ml of the medium of a 7-day-old cell culture was replaced by fresh medium. Four milliliters of the cell culture were incubated with DMSO or 10 μM E-64d (Sigma) or epoxomicin (BIOMOL) for 30 min in a six-well plate under gentle shaking. Subsequently, labeling occurred for two more hours by adding 2 μM MV151. Cells were washed with Honda buffer [25 g L^{-1} Ficoll 400 (Sigma); 50 g L^{-1} Dextran T40 (GE Healthcare Life Sciences); 0.4 M sucrose; 25 mM TRIS pH 7.4; 10 mM $MgCl_2$; protease inhibitor cocktail (Sigma); and 5 mM DTT] and homogenized in a mortar in 5 ml Honda buffer. The extract was centrifuged gently at 201 ***g*** through a 62-μm nylon mesh, and 0.5% Triton X-100 was added to the filtrate. After a 15-min incubation on ice, a 200 μl sample was taken as total extract (T), and mixed with 80 μl gel-loading buffer. The extract was centrifuged (5 min at 1500 ***g***) and a 200 μl sample was taken from the supernatant as a ND extract and mixed with 80 μl gel-loading buffer. The pellet was washed twice with 3 ml Honda buffer containing 0.1% Triton X-100 and dissolved in 200 μl gel loading buffer, resulting in a NE fraction that is 20-fold more concentrated than the NE and T fractions. Proteins were separated on protein gels and detected by fluorescent scanning and using antibodies for PBA1, PEPC and histone, as previously described (Noel *et al.*, 2007; Cheng *et al.*, 2009).

Affinity purification and identification of labeled proteins

Proteins of 8-week-old plants were extracted by grinding rosette leaves of 10 plants in an ice-cold mortar with 3 ml water and subsequent centrifugation for 10 min at 20 000 ***g***. Two and a half milliliters of supernatant at ~4 mg ml^{-1} was labeled with 20 μM BioVS in 50 mM TRIS buffer (pH 9) and 1 mM DTT for 4 h at room temperature under gentle agitation. The labeled leaf extracts were applied to PD-10 size exclusion columns (Bio-Rad, http://www.bio-rad.com/) to remove unlabeled probe. Desalted samples were incubated with 100 μl of streptavidin agarose beads (Pierce, http://www.piercenet.com/) for 1 h at room temperature under gentle agitation. Streptavidin agarose beads were collected by centrifuging for 10 min at 3000 ***g*** and washing twice with 0.1% SDS, twice with 6 M urea, once with 50 mM TRIS (pH 8) containing 1% Triton X-100, once with 1% Triton X-100, and once with water, then boiled in 30 μl of 2 × SDS-PAGE loading buffer containing β-mercaptoethanol. Affinity-purified proteins were separated on 12% one-dimensional SDS gel and stained with Coomassie (Imperial Protein Stain, Pierce). The specific band was excised from the Coomassie-stained gel and subjected to in-gel tryptic digestion and subsequent MS analysis.

The relevant bands visualized on a one-dimensional SDS gel were robotically picked as rows of 1.2-mm spots (Proteineer spII, Bruker, http://www.bruker.com/) and tryptically digested in-gel (PROTEINEERdp, Bruker). The digests were spotted onto Bruker AnchorChip targets for subsequent matrix assisted laser desorption/ionization-time of flight (MALDI-TOF) analysis. Peptide-mass fingerprints were taken with a Bruker Ultraflex III MALDI TOF/TOF MS, and the resulting spectra were processed in FlexAnalysis 3.0 (Bruker). Peak files were used to identify the corresponding proteins in the ProteinScape 1.3 database system (Protagen, http://www.protagen.de/), which triggered Mascot (Matrix Science, http://www.matrixscience.com/) searches. PBB1 (At3g27430), PBE1 (At1g13060) and PBA1 (At4g31300) were identified on the basis of peptide mass fingerprints.

ACKNOWLEDGEMENTS

We would like to thank Dr Jane Parker for suggestions and for providing seeds of the npr1-1 and PEPC and His antibodies; Anne Harzen for technical assistance; Dr Ana Garcia for help with nuclear fractionation experiments; Zheming Wang for drawing structures; Tong Lin for providing BTH, and Dr Reka Toth for statistical analysis. This work was financially supported by the Max Planck Society, the International Max Planck Research School (IMPRS), Deutsche Forschungsgemeinschaft (DFG projects HO 3983/4-1 and SCHM 2476/2-1), the Netherlands Organisation for Scientific Research (NWO) and the Netherlands Genomics Initiative (NGI) and Deutscher Akademischer Austausch Dienst (DAAD).

SUPPORTING INFORMATION

Additional Supporting Information may be found in the online version of this article:

Figure S1. Time course of MV151 labeling.

Figure S2. Concentration dependence of MV151 labeling.

Figure S3. pH dependence of MV151 labeling.

Figure S4. The reducing agent DTT increases labeling of some proteins.

Figure S5. Labeling is affected by SDS at different concentrations.

Figure S6. Adding ATP during or after extraction does not affect labeling.

Figure S7. Benzothiadiazole (BTH) treatment does not affect PBA1 subunit levels.

Figure S8. Benzothiadiazole (BTH) treatment increases the proportion of active proteasomes.

Please note: As a service to our authors and readers, this journal provides supporting information supplied by the authors. Such materials are peer-reviewed and may be re-organized for online delivery, but are not copy-edited or typeset. Technical support issues arising from supporting information (other than missing files) should be addressed to the authors.

REFERENCES

Basset, G., Raymond, P., Malek, L. and Bouquisse, R. (2002) Changes in the expression and the enzymatic properties of the 20S proteasome in sugar-starved maize roots. Evidence for an in vivo oxidation of the proteasome. *Plant Physiol.* **128**, 1149–1162.

Bonneau, L., Ge, Y., Drury, G.E. and Gallois, P. (2008) What happened to plant caspases? *J. Exp. Bot.* **59**, 491–499.

Cheng, Y.T., Germain, H., Wiermer, M. *et al.* (2009) Nuclear pore complex component MOS7/Nup88 is required for innate immunity and nuclear accumulation of defense regulators in Arabidopsis. *Plant Cell*, **21**, 2503–2516.

Cravatt, B.F., Wright, A.T. and Kozarich, J.W. (2008) Activity-based protein profiling: from enzyme chemistry to proteomic chemistry. *Annu. Rev. Biochem.* **77**, 838–414.

Dick, T.P., Nussbaum, A.K., Deeg, M. *et al.* (1998) Contribution of proteasomal β-subunits to the cleavage of peptide substrates analyzed with yeast mutants. *J. Biol. Chem.* **273**, 25637–25646.

Dietrich, R., Ploss, K. and Heil, M. (2004) Constitutive and induced resistance to pathogens in *Arabidopsis thaliana* depends on nitrogen supply. *Plant Cell Environ.* **27**, 896–906.

Drews, O., Wildgruber, R., Zong, C., Sukop, U., Nissum, M., Weber, G., Gomes, A.V. and Ping, P. (2007) Mammalian proteasome subpopulations with distinct molecular compositions and proteolytic activities. *Mol. Cell Proteomics*, **6** (11), 2021–2031.

van Esse, H.P., van't Klooster, J.W., Bolton, M.D., Yadeta, K.A., van Baarlen, P., Boeren, S., Vervoort, J., de Wit, P.J.G.M. and Thomma, B.P.H.J. (2008) The *Cladosporium fulvum* virulence protein Avr2 inhibits host proteases required for basal defense. *Plant Cell*, **20**, 1948–1963.

Gilroy, E., Hein, I., van der Hoorn, R.A.L. *et al.* (2007) Involvement of cathepsin B in the plant disease resistance hypersensitive response. *Plant J.* **52**, 1–13.

Goldberg, A.L., Cascio, P., Saric, T. and Rock, K.L. (2002) The importance of the proteasome and subsequent proteolytic steps in the generation of antigenic peptides. *Mol. Immunol.* **39**, 147–164.

Greenbaum, D., Medzihradszky, K.F., Burlingame, A. and Bogyo, M. (2000) Epoxide electrophiles as activity-dependent cysteine protease profiling and discovery tools. *Chem. Biol.* **7**, 569–581.

Groll, M., Ditzel, L., Löwe, J., Stock, D., Bochtler, M., Bartunik, H.D. and Huber, R. (1997) Structure of 20S proteasome from yeast at 2.4Å resolution. *Nature*, **386**, 463–471.

Groll, M., Schellenberg, B., Bachmann, A.S., Archer, C.R., Huber, R., Powell, T.K., Lindow, S., Kaiser, M. and Dudler, R. (2008) A plant pathogen virulence factor inhibits the eukaryotic proteasome by a novel mechanism. *Nature*, **10**, 755–758.

Hatsugai, N., Iwasaki, S., Tamura, K., Kondo, M., Fuji, K., Ogasawara, K., Nishimura, M. and Hara-Nishimura, I. (2009) A novel membrane-fusion-mediated plant immunity against bacterial pathogens. *Gene Dev.* **23**, 2449–2454.

Heinemeyer, W., Fischer, M., Krimmer, T., Stachon, U. and Wolf, D.H. (1997) The active sites of the eukaryotic 20S proteasome and their involvement in subunit precursor processing. *J. Biol. Chem.* **272**, 25200–25209.

van der Hoorn, R.A.L., Leeuwenburgh, M.A., Bogyo, M., Joosten, M.H.A.J. and Peck, S.C. (2004) Activity profiling of papain-like cysteine proteases in plants. *Plant Physiol.* **135**, 1170–1178.

Kaschani, F., Verhelst, S.H.L., van Swieten, P.F., Verdoes, M., Wong, C.S., Wang, Z., Kaiser, M., Overkleeft, H.S., Bogyo, M. and van der Hoorn, R.A.L. (2008) Minitags for small molecules: detecting targets of reactive small molecules in living plant tissues using 'click chemistry'. *Plant J.* **57**, 373–385.

Kessler, B.M., Tortorella, D., Altun, M., Kisselev, A.F., Fiebiger, E., Hekking, B.G., Ploegh, H.L. and Overkleeft, H.S. (2001) Extended peptide-based inhibitors efficiently target the proteasome and reveal overlapping specificities of the catalytic β-subunits. *Chem. Biol.* **8**, 913–929.

Kobe, B. and Kemp, B.E. (1999) Active-site-directed protein regulation. *Nature*, **402**, 373–376.

Kohler, A., Schwindling, S. and Conrath, U. (2002) Benzothiadiazole-induced priming for potentiated responses to pathogen infection, wounding, and infiltration of water into leaves requires the *NPR1/NIM1* gene in Arabidopsis. *Plant Physiol.* **128**, 1046–1056.

Kurepa, J. and Smalle, J.A. (2008) Structure, function and regulation of plant proteasomes. *Biochimie*, **90**, 324–335.

Martinez, D.E., Bartoli, C.G., Grbic, V. and Guiamet, J.J. (2007) Vacuolar cysteine proteases of wheat (*Triticum aestivum* L.) are common to leaf senescence induced by different factors. *J. Exp. Bot.* **58**, 1099–1107.

May, M.J. and Leaver, C.J. (1993) Oxidative stimulation of glutathione synthesis in *Arabidopsis thaliana* suspension cultures. *Plant Physiol.* **103**, 621–627.

Meng, L., Mohan, R., Kwok, B.H.B., Elofsson, M., Sin, N. and Crews, C.M. (1999) Epoxomicin, a potent and selective proteasome inhibitors, exhibits *in vivo* anti-inflammatory activity. *Proc. Natl Acad. Sci. USA*, **96**, 10403–10408.

Noel, L.D., Cagna, G., Stuttmann, J., Wirthmuller, L., Betsuyaku, S., Witte, C.-P., Bhat, R., Pochon, N., Colby, T. and Parker, J.E. (2007) Interaction between SGT1 and cytosolic/nuclear HSC70 chaperones regulates Arabidopsis immune responses. *Plant Cell*, **19**, 4061–4076.

Powers, J.C., Asgian, J.L., Ekici, O.D. and James, K.E. (2002) Irreversible inhibitors of serine, cysteine, and threonine proteases. *Chem. Rev.* **102**, 4639–4750.

von Rad, U., Mueller, M.J. and Durner, J. (2005) Evaluation of natural and synthetic stimulants of plant immunity by microarray technology. *New Phytol.* **165**, 191–202.

Rock, K.L., Gramm, C., Rothstein, L., Clark, K., Stein, R., Dick, L., Hwang, D. and Goldberg, A.L. (1994) Inhibitors of the proteasome block the degradation of most cell proteins and the generation of peptides presented on MHC class I molecules. *Cell*, **78**, 761–771.

Rooney, H., van 't Klooster, J., van der Hoorn, R.A.L., Joosten, M.H.A.J., Jones, J.D.G. and de Wit, P.J.G.M. (2005) Cladosporium Avr2 inhibits tomato Rcr3 protease required for Cf-2-dependent disease resistance. *Science*, **308**, 1783–1789.

Shabab, M., Shindo, T., Gu, C., Kaschani, F., Pansuriya, T., Chintha, R., Harzen, A., Colby, T., Kamoun, S. and Van der Hoorn, R.A.L. (2008) Fungal effector protein AVR2 targets diversifying defense-related Cys proteases of tomato. *Plant Cell*, **20**, 1169–1183.

Song, J., Win, J., Tian, M., Schornack, S., Kaschani, F., Muhammad, I., van der Hoorn, R.A.L. and Kamoun, S. (2009) Apoplastic effectors secreted by two unrelated eukaryotic plant pathogens target the tomato defense protease Rcr3. *Proc. Natl Acad. Sci. USA*, **106**, 1654–1659.

Spoel, S.H., Mou, Z., Tada, Y., Spivey, N.W., Genschik, P. and Dong, X. (2009) Proteasome-mediated turnover of the transcription coactivator NPR1 plays dual roles in regulating plant immunity. *Cell*, **137**, 860–872.

Sullivan, J.A., Shirasu, K. and Deng, X.W. (2003) The diverse roles of ubiquitin and the 26S proteasome in the life of plants. *Nat. Rev. Genet.* **4**, 948–958.

Suty, L., Lequeu, J., Lancon, A., Etienne, P., Petitot, A.S. and Blein, J.P. (2003) Preferential induction of 20S proteasome subunits during elicitation of plant defense reactions: towards the characterization of 'plant defense proteasomes'. *Int. J. Biochem. Cell Biol.* **35**, 637–650.

Tian, M., Win, J., Song, J., van der Hoorn, R.A.L., van der Knaap, E. and Kamoun, S. (2007) A *Phytophthora infestans* cystatin-like protein interacts with and inhibits a tomato papain-like apoplastic protease. *Plant Physiol.* **143**, 364–277.

Verdoes, M., Florea, B.I., Menendez-Benito, V. *et al.* (2006) A fluorescent broad-spectrum proteasome inhibitor for labeling proteasomes *in vitro* and *in vivo*. *Chem. Biol.* **13**, 1217–1226.

Wang, Z., Gu, C., Colby, T., Shindo, T., Balamurugan, R., Waldmann, H., Kaiser, M. and van der Hoorn, R.A.L. (2008) Beta-lactone probes identify a papain-like peptide ligase in *Arabidopsis thaliana*. *Nat. Chem. Biol.* **4**, 557–563.

Wilk, S. and Orlowski, M. (1980) Cation-sensitive neutral endopeptidase: isolation and specificity of the bovine pituitary enzyme. *J. Neurochem.* **35**, 1172–1182.

Yamada, K., Matsushima, R., Nishimura, M. and Hara-Nishimura, I. (2001) A slow maturation of a cysteine protease with a granulin domain in the vacuoles of senescing Arabidopsis leaves. *Plant Physiol.* **127**, 1626–1634.

Yang, P., Fu, H., Walker, J., Papa, C.M., Smalle, J., Ju, Y.M. and Vierstra, R.D. (2004) Purification of the Arabidopsis 26S proteasome. *J. Biol. Chem.* **279**, 6401–6413.

Zimmermann, P., Hirsch-Hoffmann, M., Hennig, L. and Gruissem, W. (2004) GENEVESTIGATOR: Arabidopsis microarray database and analysis toolbox. *Plant Physiol.* **136**, 2621–2632.

